

Sequential nonadiabatic excitation of large molecules and ions driven by strong laser fieldsAlexei N. Markevitch,¹ Dmitri A. Romanov,² Stanley M. Smith,³ H. Bernhard Schlegel,³
Misha Yu. Ivanov,⁴ and Robert J. Levis^{1,*}¹*Department of Chemistry, Center for Advanced Photonics Research, Temple University, Philadelphia, Pennsylvania 19122, USA*²*Department of Physics, Center for Advanced Photonics Research, Temple University, Philadelphia, Pennsylvania 19122, USA*³*Department of Chemistry, Wayne State University, Detroit, Michigan 48202, USA*⁴*Steacie Institute for Molecular Sciences, NRC Canada, 100 Sussex Drive, Ottawa, Canada ON K1A 0R6*

(Received 26 August 2003; published 13 January 2004)

Electronic processes leading to dissociative ionization of polyatomic molecules in strong laser fields are investigated experimentally, theoretically, and numerically. Using time-of-flight ion mass spectroscopy, we study the dependence of fragmentation on laser intensity for a series of related molecules and report regular trends in this dependence on the size, symmetry, and electronic structure of a molecule. Based on these data, we develop a model of dissociative ionization of polyatomic molecules in intense laser fields. The model is built on three elements: (i) nonadiabatic population transfer from the ground electronic state to the excited-state manifold via a doorway (charge-transfer) transition; (ii) exponential enhancement of this transition by collective dynamic polarization of all electrons, and (iii) sequential energy deposition in both neutral molecules and resulting molecular ions. The sequential nonadiabatic excitation is accelerated by a counterintuitive increase of a large molecule's polarizability following its ionization. The generic theory of sequential nonadiabatic excitation forms a basis for quantitative description of various nonlinear processes in polyatomic molecules and ions in strong laser fields.

DOI: 10.1103/PhysRevA.69.013401

PACS number(s): 33.80.Rv, 82.50.Pt

I. INTRODUCTION

The interaction of a strong nonresonant laser field with a molecule is governed by the interplay of electron system characteristics and the laser pulse parameters (duration, intensity, frequency, etc.). All nonresonant interactions can be classified as either adiabatic, when the molecular energy states follow the field without interstate transitions, or nonadiabatic, when the interstate transitions occur. Adiabatic nonresonant interaction results in single [1–3] or multiple [4,5] ionization. This process is described by quasistatic theories of tunnel ionization [1,6]. A single tunnel ionization event generally leads to the formation of an intact molecular ion [2,3] in its ground electronic state; multiple electron removal results in energetic dissociation known as Coulomb explosion [7,8]. Nonadiabatic molecule-laser interaction results in all other possible outcomes, such as nonresonant electronic excitation [9], internal conversion [10,11], fragmentation to neutral products [3], dissociative ionization [12,13], nuclear rearrangement [14], etc. Utilization of these processes requires an understanding of physical mechanisms that determine the transition from the adiabatic to the nonadiabatic coupling regime. In particular, an adequate description of the energy deposition into polyatomic molecules, leading to their fragmentation, is crucial for predicting and controlling fragmentation patterns [14–16].

The exploration of nonadiabatic electron dynamics in strong fields has a long history, which starts with atoms, continues with small (diatomic) molecules, and culminates in large (polyatomic) molecules that are the subject of this publication. At each of these hierarchical levels, the complexity

of the system increases dramatically, requiring a “quantum leap” in understanding and in the principles of description.

Strong-field atomic ionization is usually described in the long-wavelength case using single active electron (SAE) tunnel ionization theories [17–19]. Indeed, in the quasistatic limit, nonadiabatic excitation of atoms can be ignored. However, at shorter wavelengths (in the optical region), nonadiabatic excitation of atoms does occur and may be enhanced and modified by electron correlation effects even for two-electron atoms [20]. For multielectron atoms, large populations of electronically excited atoms have been detected in the above-threshold ionization (ATI [21]) photoelectron spectra following nonresonant strong field atomic excitation using a 620-nm laser [22]. Strong-field nonadiabatic electronic excitation of atoms has been explained using the paradigm of transient multiphoton resonances between dynamically Stark-shifted ground and excited electronic states [23–25].

Whereas nonadiabatic transitions are important in strong-field electron dynamics of atoms, they should play an even more important role in molecular excitation. This is because molecules are typically larger and more complex than atoms; that is, they have more complex and subtle electronic structure (in particular, lower symmetry). In addition, molecules have nuclear degrees of freedom (rotational and vibrational) and can undergo internal conversion or dissociate. For molecules, the variety of competing outcomes of nonadiabatic excitation must be greatly increased, while the utility of both SAE and quasistatic approaches is greatly reduced.

The coupling of a multielectron system with the laser field is significantly affected by the electronic structure of the system. The electronic structures of atoms and molecules differ qualitatively: molecules possess a new (compared to atoms) feature of electronic structure—charge-transfer electronic

*Author to whom correspondence should be addressed.

states, $|CT\rangle$. As will be seen in the following sections, these states play an important role in the molecules we investigate; this is why we address them here in some detail. A $|CT\rangle$ state has been defined [26] for symmetric diatomic molecules as a state having the electronic charge density primarily localized to one of the atoms. Should a neutral diatomic molecule undergo dissociation from a $|CT\rangle$ state, the result will be a pair of ions rather than neutral fragments. A CT electronic transition couples a symmetric electronic state (typically the ground state, $|g\rangle$) with a $|CT\rangle$ state. (In the smallest diatomic molecule, H_2 , the CT electronic transition couples the ground $^1\Sigma_g^+$ state with the ion pair state $^1\Sigma_u^+$, the excited state corresponding to dissociation into H^- and H^+ .) Qualitatively, the transition dipole moments for CT transitions are proportional to the distance over which the charge is transferred. Thus, in the case of a diatomic molecule, the transition dipole moment grows with the internuclear separation R ; in the limit of large R , it asymptotically approaches $eR/2$ [26].

The role of $|CT\rangle$ states in the dissociation dynamics of diatomic molecular ions in intense infrared laser fields has been pointed out in Ref. [27]. The electron dynamics of small (diatomic and small polyatomic) molecules has been shown theoretically [28–30] to become highly nonadiabatic in strong laser fields. This nonadiabatic dynamics leads to CT localization when the dissociating molecule is stretched to a critical internuclear distance (approximately two to three times larger than the equilibrium distance). Evidence for this nonadiabatic localization of the electronic wave function can be found in enhanced ionization rate [30], generation of even harmonics from centrosymmetric ions [31], and in the asymmetric charge distribution of ionic fragments [32,33].

In larger molecules, $|CT\rangle$ states can also provide a natural framework for qualitative understanding of the large-amplitude charge motion among the atoms of a molecule or a molecular ion in strong oscillating electric fields. Even in a medium-size molecule (CH_2I_2), the critical distance for CT localization is already achieved in the equilibrium nuclear geometry [34]. Yet larger spatial dimensions of a molecule should further enhance the role of $|CT\rangle$ states in nonadiabatic electronic excitations.

Polyatomic molecules are different from small (diatomic) molecules in one obvious aspect: size. The larger size of a molecule not only increases the number of electrons but also the spatial extent of its electronic states. Both these factors are likely to facilitate nonadiabatic dynamics in a strong laser field. Indeed, significant effects of nonadiabatic dynamics on the ionization and dissociation of polyatomic molecules can be discerned from experiments on a series of related organic molecules of increasing size. Both increasing laser frequency [35] and pulse amplitude [13] lead to more extensive fragmentation in molecules of a given size. At the same time, similar fragmentation channels are activated at lower laser intensities for molecules of increasing size at a given laser frequency. To understand physical mechanisms for the transition from adiabatic to nonadiabatic coupling regimes as a function of laser intensity, frequency, and pulse duration, we need analytical models that capture the most salient features of the excitation process.

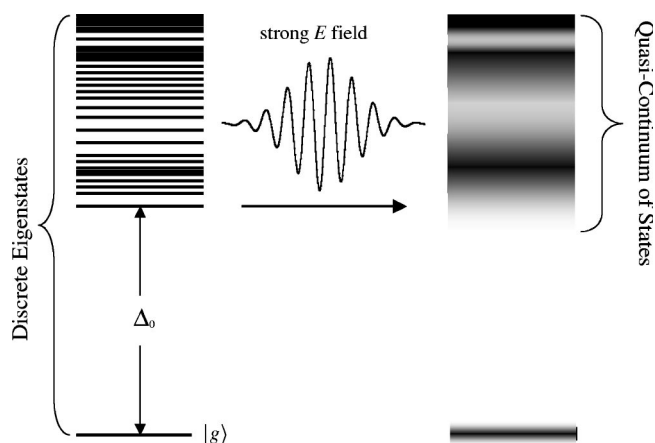


FIG. 1. Formation of quasicontinuum of electronic states in strong laser field. On the left: discrete electronic molecular eigenstates in the field-free case. On the right: strong laser field merges the electronic states in the excited-state manifold into a quasicontinuum.

A recently proposed model of strong-field energy absorption by electrons in large polyatomic molecules [35] predicts that nonadiabatic excitation should generally intensify with molecular size, laser field frequency, and amplitude. In this model, a strong laser field merges all of the electronic states of a molecule into a quasicontinuum (QC). Within this QC, classical plasmlike energy absorption is expected, resulting eventually in ionization and fragmentation of the molecule.

This simple model, however, has not addressed the complexity of real molecules and thus has left open too many questions regarding the process and outcomes of nonadiabatic excitation. The relationship between molecular properties and mechanism of excitation is both unknown and essential for predicting the threshold for nonadiabatic transitions. As for the outcomes, it is not clear whether the nonadiabatic excitation should result in fragmentation of a molecule into neutral products, intact ionization, or dissociative ionization. These outcomes should depend on specific molecular properties, not identified by this theory.

In addition, there are unanswered fundamental questions regarding the very process of nonadiabatic excitation via QC. According to Ref. [35], the QC is formed due to electronic state broadening caused by efficient nonadiabatic transitions that are saturated on the time scale of a single laser cycle for any pair of electronic states, under the condition $\mu \epsilon_0 \hbar \omega \geq \Delta^2$ (here, μ and Δ are the transition dipole moment and the transition energy; ϵ_0 and ω are the electric-field amplitude and frequency); see Fig. 1. Since the $|g\rangle$ state is normally separated from the excited-state manifold by a considerable energy gap, the mechanism of coupling of $|g\rangle$ to the QC needs to be established and utilized.

Motivated by these questions, we set out to study the mechanism of the transition from adiabatic coupling to nonadiabatic energy deposition in strong laser fields. We investigated dissociative ionization of a number of related aromatic molecules of varying molecular size and/or π -electron delocalization as a function of laser intensity. Based on these experiments, we identified key physical parameters of large

polyatomic molecules that govern this transition and developed a general theory of nonadiabatic excitation of polyatomic molecules in strong laser fields. In a recent communication [36], we introduced this theory using an opening subset of experiments. Here, we present a more complete and detailed account of this work, including new experimental data and new calculations supporting and further developing the theory of nonadiabatic excitation in polyatomic molecules and ions.

The paper is organized as follows. In Sec. II, the experimental procedure is described; in Sec. III, the experimental observations are reported; in Sec. IV, a theory corroborated by calculations to explain the observed phenomena is presented. Finally, in Sec. V, we summarize our findings, comment on the significance of the theory, and outline directions for its further development.

II. EXPERIMENTAL PROCEDURE

The extent of fragmentation observed in the ion time-of-flight mass spectra is used as a representative measure for the onset of nonadiabatic electron dynamics. Accordingly, we collected time-of-flight ion spectra of the products resulting from interaction of large organic molecules with strong-field laser pulses. The excitation source was a 10-Hz mode-locked regeneratively chirped-pulse amplified Ti:sapphire laser similar to that described in earlier publications [37,38]. The laser produced 1.5-mJ, 60-fs pulses centered at 800 nm. Pulses were focused to a spot of $\sim 50\text{-}\mu\text{m}$ diam by a nominally 20-cm focal length lens, and intensities were calibrated by comparison to the appearance thresholds for multiply charged argon. A 1-mm aperture was placed between the ionization and detection regions in order to ensure that only ions generated in the most intense region of the laser beam were collected [39]. The Rayleigh length of the laser beam focus was ~ 3 mm. The time-of-flight ion spectra were collected as a function of the laser intensity. The laser pulses were attenuated by inserting a variable number of glass cover slides (CorningTM) in the beam path. The transmission of the cover slides, independently measured using a uv-visible spectrometer, was $\sim 92.5\%$ per slide. The average pulse energies were also measured for each spectrum using a calibrated power meter.

Ion spectra were measured using a linear one-meter time-of-flight mass spectrometer in dual slope continuous extraction mode. Solid samples were allowed to sublime directly into vacuum to attain a pressure of $\sim 1 \times 10^{-6}$ Torr with a background pressure for the spectrometer of $\sim 1 \times 10^{-8}$ Torr. Benzene was delivered through a controlled leak valve. The low working pressure insures that no space-charge interactions affect the excitation dynamics. The reported ion spectra are averages of 250 single shot acquisitions. All experiments were performed using linearly polarized laser pulses with the direction of electric-field polarization aligned with the direction of ion detection in the spectrometer.

III. EXPERIMENTAL RESULTS

To establish the molecular characteristics most important in the processes of nonadiabatic excitation, we investigated

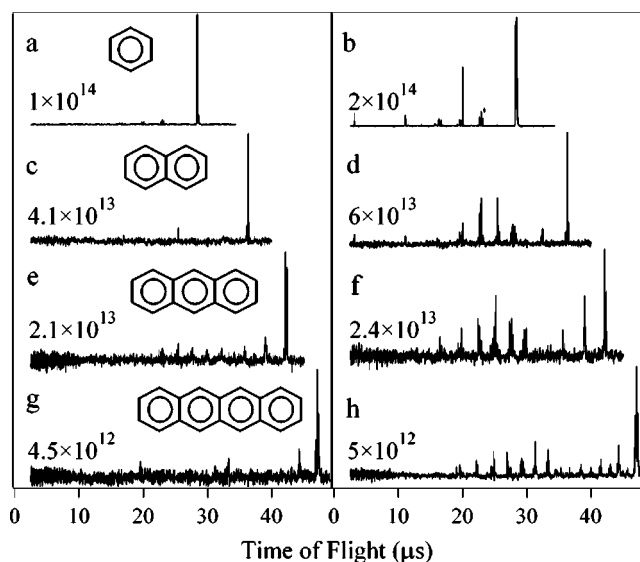


FIG. 2. Time-of-flight mass spectra of (a,b) benzene, (c,d) naphthalene, (e,f) anthracene, (g,h) tetracene, obtained using 800-nm, 60-fs laser pulses. The laser intensities in W cm^{-2} are shown for each spectrum.

the dissociative ionization for two series of related molecules as a function of laser intensity. In series 1 (benzene, naphthalene, anthracene, and tetracene), shown in Fig. 2, the characteristic length of the aromatic molecules increases from benzene to tetracene, along with the extent of π -electron delocalization that should directly affect μ and Δ for the electronic excitation from $|g\rangle$. In series 2, shown in Fig. 3 [1,2,3,4,5,6,7,8-octahydroanthracene (OHA), 9,10-dihydroanthracene (DHA), and anthracene], the characteristic lengths are similar but the extent of π delocalization nevertheless increases from OHA to anthracene, with an increasing number of unsaturated aromatic rings. The diversity of the molecules within and between the two series allows us to independently verify the constituent elements of our theoretical model and investigate the characteristic parameters that determine details of the nonadiabatic processes.

The mass spectra were obtained at laser intensities between $0.1 \times 10^{13} \text{ W cm}^{-2}$ and $25.0 \times 10^{13} \text{ W cm}^{-2}$. For series 1, the extent of fragmentation increases at all laser intensities with increasing molecular size. The spectra are dominated by a parent molecular ion at the lowest laser intensities, Figs. 2(a)–2(d). As the laser intensity is increased, fragments emerge at increasing rate, starting at some onset intensity value, I_{fragm} . (We define I_{fragm} as the point where the five-point running average value of this ratio exceeds the background value by two standard deviations.) Finally, the fragmentation saturates at higher intensities. Figures 2(e)–2(h) shows the ion spectra at laser intensities greater than I_{fragm} but below saturation.

For the three larger molecules—naphthalene, anthracene, and tetracene—there is a marked threshold, I_{fragm} , for the onset of extensive fragmentation. The transition from limited to extensive fragmentation requires only a small change in laser intensity (10–20%). For the smallest molecule, benzene, this transition requires a relatively large increase in

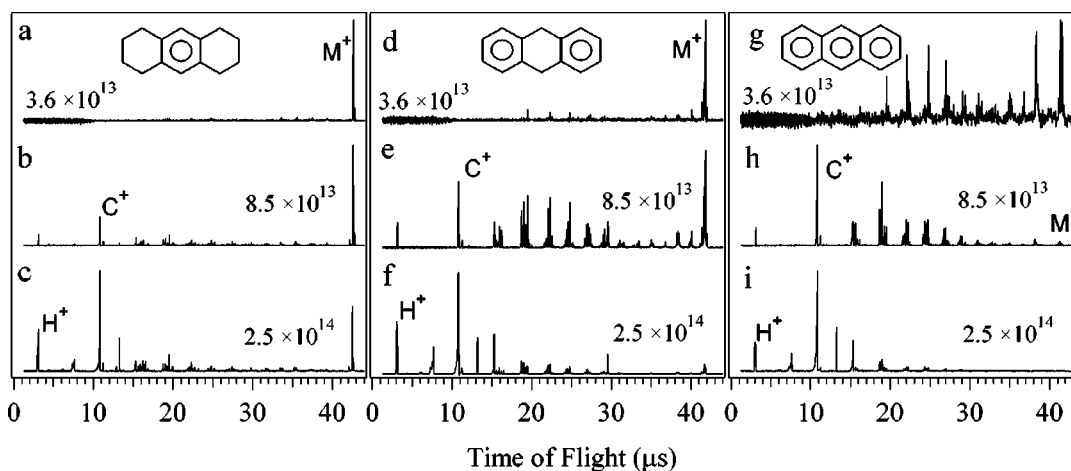


FIG. 3. Time-of-flight mass spectra of (a,b,c) OHA, (d,e,f) DHA, (g,h,i) anthracene, obtained using 800-nm, 60-fs laser pulses. The laser intensities in W cm^{-2} are shown for each spectrum.

laser intensity (from 1.0 to $\sim 2.0 \times 10^{14} \text{ W cm}^{-2}$). From the conventional perturbative picture, this observation is counterintuitive. Indeed, for larger molecules (tetracene, anthracene) the number of photons required for electronic excitation decreases and thus the intensity dependence should be of lower order than for smaller molecules (naphthalene, benzene). This is contrary to our observation. The data shown in Fig. 2 reveal that the sensitivity of the molecular fragmentation process to the laser intensity increases for molecules of larger size.

We next examine the conditions for the onset of extensive fragmentation for the series of molecules of similar size but varying extent of π delocalization, series 2. Time-of-flight mass spectra for OHA, DHA, and anthracene measured at laser intensities of 3.6 , 8.5 , and $25.0 \times 10^{13} \text{ W cm}^{-2}$ are shown in Figs. 3(a)–3(c), 3(d)–3(f), and 3(g)–3(i), respectively. Again, the extent of fragmentation increases with increasing π -electron delocalization (OHA to DHA to anthracene) at all laser intensities. Furthermore, the spectra of OHA have a more intense parent ion in comparison with the spectra of DHA and anthracene at all intensities. The lack of fragmentation in the OHA is remarkable given the fact that OHA has the largest fraction of saturated single σ -type C—C bonds. Such bonding typically has a reduced dissociation energy in comparison to aromatic π bonds and results in enhanced dissociative ionization during strong-field excitation [3].

To quantitatively define the value of I_{fragm} , we plot the ratio of fragment ion signal to the total ion signal versus the laser intensity. These data are shown for series 1 in Fig. 4(a) and for series 2 in Fig. 4(b). We define I_{fragm} as the laser intensity at which the five-point running average value of this ratio exceeds the background value by two standard deviations. The I_{fragm} values reported in Table I reveal that the onset of extensive dissociation occurs at lower laser intensities with increasing molecular size for series 1 and increasing degree of unsaturation in series 2.

IV. DISCUSSION

The popular SAE quasistatic atomic [17–19] and molecular [37,40,6] models of strong-field ionization disregard the

existence of the excited electronic states of these systems. Such models address tunnel ionization in the low-frequency quasistatic limit, when the photon energy is much smaller than the ionization potential of a system, $\hbar\omega \ll \text{IP}$. At such low frequencies, the characteristic amplitude of free electron motion in the oscillating electric field, $a_{\text{osc}} = e\varepsilon_0/m_e\omega^2$, is much larger than the characteristic size of the molecule, L . (Here, e is the electron charge, m_e is the electron mass, and ε_0 and ω are the laser field amplitude and frequency.) Under

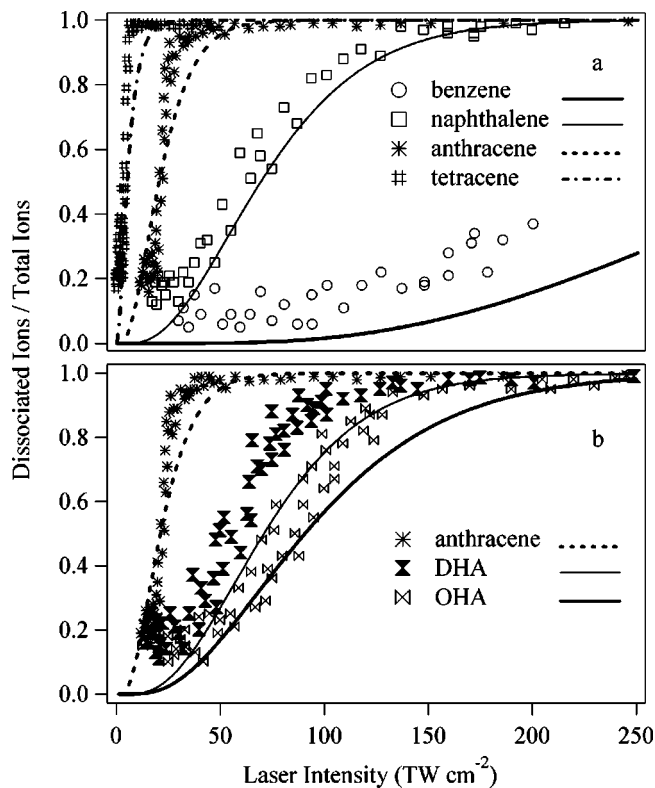




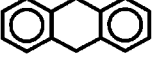
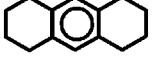


FIG. 4. Fragmentation fraction and NMED calculation: (a) BNAT series; (b) anthracene-DHA-OHA series. The curves show the calculated fraction of the molecular ions excited nonadiabatically by the end of a laser pulse (integrated conditional probabilities of two-stage nonadiabatic excitation).

TABLE I. Measured and calculated properties of the molecules used in this study. The characteristic transition energies, transition dipole moments, and dynamic polarizabilities of the ground states of neutral molecules and molecular ions were calculated using the GAUSSIAN G01 (development version) computer program using the B3LYP density-functional method with a 6-31+G(d) basis set.

Molecular name and formula	Chemical structure	I_{fragm} $\times 10^{13}$ ($W\text{ cm}^{-2}$)	Δ_0 $ g\rangle \rightarrow DS\rangle$ neutral/ion, (eV)	μ $ g\rangle \rightarrow DS\rangle$ neutral/ion, (e Å)	$P_{ g\rangle \rightarrow DS\rangle}$ neutral two-state	$\alpha_g(800\text{ nm})$ neutral/ion, ($e\text{ Å}^2\text{ V}^{-1}$)	$\mu^2/\Delta_0\alpha_g$ neutral/ion, (%)
Benzene, C_6H_6		16 ± 3	7.00 (7.23)	2.01 (0.905)	3.0×10^{-2}	0.779 (0.679)	74 (17)
Naphthalene, $C_{10}H_8$		4.1 ± 0.5	5.88 (5.90)	1.57 (1.41)	2.0×10^{-3}	1.70 (2.25)	42 (15)
Anthracene, $C_{14}H_{10}$		2.1 ± 0.2	5.17 (5.13)	2.10 (1.91)	6.5×10^{-3}	3.02 (5.13)	28 (14)
Tetracene, $C_{18}H_{12}$		0.45 ± 0.05	4.65 (4.59)	2.58 (2.35)	7.8×10^{-4}	4.75 (15.67)	30 (7.7)
9,10- dihydroanthracene, $C_{14}H_{12}$ (DHA)		4.0 ± 0.5	5.73 (5.9)	1.40 (1.53)	1.2×10^{-3}	2.07 (1.93)	16.5 (21)
1,2,3,4,5,6,7,8- octahydroanthracene, $C_{14}H_{18}$ (OHA)		5.9 ± 0.5	6.14 (6.37)	0.711 (1.04)	3.8×10^{-6}	2.11 (2.72)	4 (6.3)

such conditions, dynamic polarization of a molecule is expected to be adiabatic. As a result, the polarized electrons spend most of the laser half-cycle localized at one side of the molecule from where the quasistatic tunneling occurs. Qualitatively, the potential barrier for this tunneling ionization is reduced by the polarization energy of the SAE, i.e., by the energy decrease at the side of the molecule, $\sim e\epsilon_0 L/2$. The quasistatic molecular structure-based model [1,37] accounts for this effect and, in keeping with experimental results [1,3,13,41], predicts increasing ionization rate with increasing spatial extent of a molecule. Within this adiabatic framework, the only outcome of the laser-field action can be formation of ground-state singly or multiply charged parent ions. Any fragmentation can only be caused by Coulomb repulsion following multiple ionization.

In contrast to this picture, a growing body of experimental data [12,13,35] suggests that in polyatomic molecules, nonadiabatic coupling into internal degrees of freedom occurs in the initial stages of strong-field excitation, i.e., when the condition $a_{osc} \gg L$ is not yet satisfied. For example, in Fig. 5 we compare the values of a_{osc} at the fragmentation threshold with the size of the four polyatomic molecules used in this study. The smallest molecule, benzene, undergoes extensive fragmentation at $a_{osc} \gg L$. Molecules of intermediate size, namely naphthalene and anthracene, fragment at $a_{osc} \sim L$. The largest molecule, tetracene, fragments in the regime $a_{osc} < L$. This shows that the SAE models of adiabatic tunnel ionization do not adequately describe the electron dynamics of polyatomic molecules at these laser intensities and frequencies.

To explain the formation of repulsive excited states of molecular ions, it was suggested [35] that the strong electric field of a laser merges all of the electronic states of a mol-

ecule into a quasicontinuum, QC. The delocalized electrons quiver inside a molecule within the QC, with the average energy on the order of the ponderomotive potential, $U_p = (e^2 \epsilon_0^2 / 4m_e \omega^2)$. Any scattering in the presence of the field, either from corrugation of the potential or from other electrons, leads to absorption/emission of energy $\sim U_p$. This phenomenon is similar to laser-assisted bremsstrahlung [42]. In this picture, strong nonresonant excitation should begin at laser field intensities, when U_p approaches the characteristic spacing of electronic energy levels and forces the QC forma-

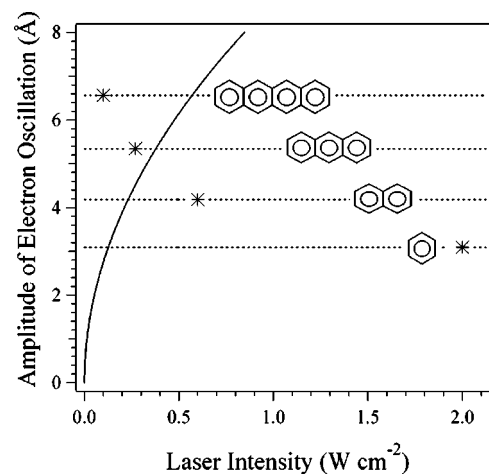


FIG. 5. The amplitude of oscillation of a free electron as a function of laser intensity of 800-nm laser field (solid curve). The markers denote the laser intensity for the onset of extensive fragmentation of the molecules in the BNAT series as a function of the molecular size. The dashed lines are drawn at the level corresponding to half the characteristic length of each molecule.

tion in the system [35]. However, as we have already mentioned in the Introduction, this simple model does not concur with the results of our experiments.

As we discuss in more detail in the rest of this section, in order to be consistent and to comprehensively accommodate the experimental results, a model of dissociative ionization caused by nonadiabatic excitation should be based on three major elements: (i) the doorway state |DS⟩ for the nonadiabatic transition into the excited-states manifold; (ii) multi-electron polarization of the |*g*⟩ and |DS⟩; and (iii) sequential energy deposition in the neutral molecules and corresponding molecular ions. In this model, the first excitation stage leads to ionization; the second (and subsequent) stages result in the molecular ion fragmentation. In the following subsections, we will introduce these three elements, concluding with a demonstration that the full-fledged model allows calculation of the fragmentation probabilities that agree quantitatively with the experimental data.

The modeling and calculations for both neutral molecules and molecular ions are performed for the equilibrium internuclear geometry of neutral molecules. The laser pulses used in this work are sufficiently short (60 fs) that at the laser intensities $\leq I_{\text{fragm}}$, nuclear degrees of freedom are nearly frozen during the laser pulse. Thus, nuclear excitation can be understood in two steps: (i) during the pulse, the laser energy is nonadiabatically coupled into electronic degrees of freedom; (ii) after the laser pulse, the stored energy is available for the excitation of nuclear modes.

A. Doorway electronic states

For most polyatomic molecules (including the molecules in this study), the energy gap separating |*g*⟩ from the manifold of the excited electronic states is large in comparison with the energy-level splitting in the excited-state manifold. Indeed, the analysis of the data presented in Sec. III shows that the extensive fragmentation of these molecules actually begins when $\mu\varepsilon_0\hbar\omega \ll \Delta^2$ for the transitions from |*g*⟩ to the excited states of the molecule (see Table I). Since for these laser intensities the condition $\mu\varepsilon_0\hbar\omega \gg \Delta^2$ is satisfied for the excited-state manifold (where $\Delta \ll \hbar\omega$), we conclude that QC is formed only from excited states of the molecule, and thus the transition from |*g*⟩ to the excited quasicontinuum, |*g*⟩ → QC, is the rate-limiting step in the nonadiabatic excitation. The |*g*⟩ → QC transition must be treated separately. When this bottleneck has been overcome, nonadiabatic excitations in the QC should allow a molecule rapidly to climb the ladder of excited states and ionize. If the process is repeated in the molecular ion, the excited-states manifold of the molecular ion will be accessed. Since some of the excited electronic states of molecular ions are repulsive, dissociative ionization should result.

The natural framework for quantitative treatment of the nonresonant quasiadiabatic (Landau-Zener) transitions was provided by the Dykhne formalism [43]. In this formalism, the energy of an electronic state adiabatically follows the oscillations of the laser electric field, $\varepsilon(t) = \varepsilon_0 \sin(\omega t)$. For two eigenstates |*m*⟩ and |*n*⟩ coupled by a transition dipole μ_{mn} and separated by characteristic energy-level spacing

Δ_{mn} , the time-dependent transition energy is [44]

$$\Delta E_{|m\rangle,|n\rangle}(t) = \sqrt{\Delta_{mn}^2 + 4\mu_{mn}^2 \varepsilon^2(t)}. \quad (1)$$

The time dependence $\Delta E_{|m\rangle,|n\rangle}(t)$ induces nonadiabatic interstate transitions analogous to the semiclassical Landau-Zener transitions through an avoided crossing at $t=0$. The transition probability during one-half laser cycle is obtained as

$$P_{|m\rangle \rightarrow |n\rangle} = \exp\left[-\frac{2}{\hbar} \text{Im}\left\{\int_1^{\tau^*} \Delta E_{|m\rangle,|n\rangle}(t) dt\right\}\right]. \quad (2)$$

The upper limit in the integral, τ^* , is given by the saddle-point condition $\Delta E_{|m\rangle,|n\rangle}(\tau^*) = 0$. For the two-state model of Eq. (1), this treatment results (see the Appendix) in a half-laser cycle transition probability of

$$P_{|m\rangle \rightarrow |n\rangle} = \exp\{-\pi\Delta^2/4\hbar\omega\varepsilon_0\mu\}. \quad (3)$$

Therefore, when $\mu\varepsilon_0\hbar\omega \gg \Delta^2$, the probability for the transition will approach unity, and this transition will be rapidly saturated.

The Dykhne approach has been extensively used [45] to describe transitions to the true continuum; here we apply it to treat the |*g*⟩ → QC electronic transition coupling |*g*⟩ to the manifold of excited states of a polyatomic molecule. Unlike in the case of a true continuum, where the edge is clearly defined, here we must identify the electronic state connecting |*g*⟩ to the excited-states manifold. Though many states may be connected to |*g*⟩, the exponential dependence in Eq. (2) implies that the |*g*⟩ → QC transition occurs mainly through the state that is most strongly coupled to |*g*⟩; we call it the doorway state, |DS⟩. For a low-frequency laser field, the strength of the coupling may be defined by the dimensionless parameter $\Gamma = \mu_{ge}\varepsilon\hbar\omega/\Delta_{ge}^2$ (where μ_{ge} is the transition dipole matrix element from |*g*⟩ to the candidate excited state, and Δ_{ge} is the energy difference between these states). For $\Gamma \ll 1$, nonadiabatic excitation is negligible; when Γ approaches unity, the excitation is saturated within a few laser cycles. The |DS⟩ state is that for which Γ is the largest at a given field amplitude and frequency.

We calculated the characteristic energy-level spacings and the transition dipole moments for the electronic transitions of these molecules, using GAUSSIAN 01 (development version [46]) using B3LYP density-functional method [47–49] with a 6-31+G(d) basis set [50–54] (the details of these calculations will be published elsewhere [55]). According to these calculations, the majority of the excited states have negligibly small transition dipoles and oscillator strengths for the transition from |*g*⟩. The only two states that compete for the |DS⟩ role are the π^* state, the first excited state |1*⟩, and the lowest charge-transfer state |CT⟩. The calculations reveal that for all of the studied molecules, the values of Γ for |*g*⟩ → |CT⟩ transitions are several times larger than those for |*g*⟩ → |1*⟩ transitions, see Table I.

This situation is peculiar and distinct from the case of the transitions to the true continuum, because the |*g*⟩ → |CT⟩ transitions are much stronger than the |*g*⟩ → |1*⟩ correspond-

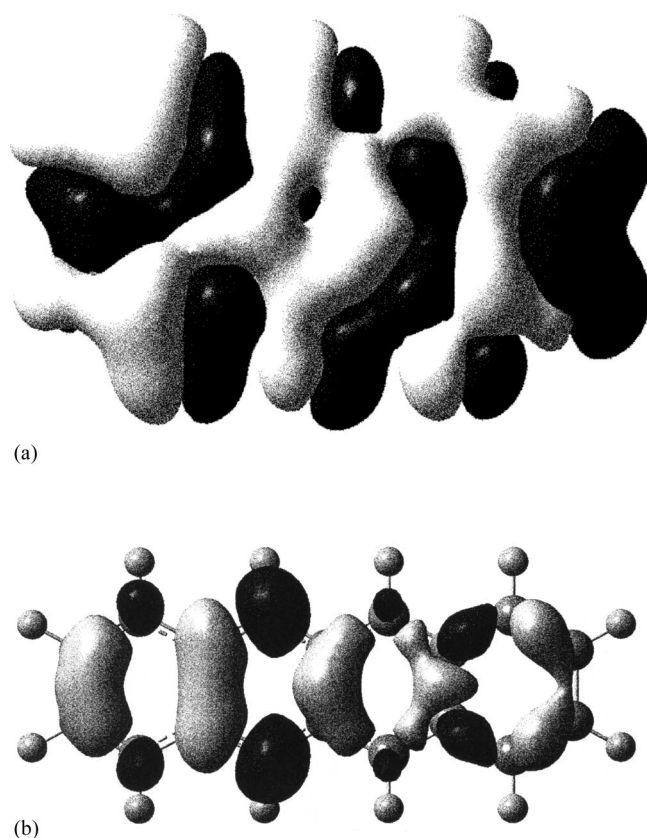


FIG. 6. The direction of transfer of electronic density during the electronic transition from the ground electronic state to the $|CT\rangle$ state of (a) neutral anthracene and (b) singly charged molecular ion of tetracene. The light-shaded and dark-shaded areas indicate the regions of decreased and increased electron density in comparison with the distribution in the ground state, respectively.

ing to $\pi \rightarrow \pi^*$ excitations, despite the fact that the latter have smaller excitation energy from $|g\rangle$. It is natural that the $|g\rangle \rightarrow |CT\rangle$ electronic transitions are most important in describing the laser/molecule coupling, governed by large-amplitude charge redistribution in the longest dimension of an extended planar molecule. We conclude that for these molecules the $|DS\rangle$ state is the lowest-energy $|CT\rangle$ state.

The graphic representation of the electron density redistribution as a result of CT electronic transition in these molecules (and their molecular ions) is illustrated in the case of tetracene in Fig. 6. (This picture of charge-transfer states has been generated using the GAUSSIAN 01 development version program.) In Fig. 6, the electron density is transferred from the light-shaded to the dark-shaded areas. Thus, the figure shows the difference between the electron densities of the $|CT\rangle$ state and the ground state, illustrating the asymmetric shift of electrons to one side of the molecule following a CT electronic transition.

Additional insight into role of $\pi \rightarrow \pi^*$ and $|g\rangle \rightarrow |CT\rangle$ transitions in the connection between the $|g\rangle$ and the excited-states manifold was obtained from a comparative study of planar and nonplanar aromatic molecules. For a planar aromatic molecule, the transition dipole moment for the $\pi \rightarrow \pi^*$ transition is perpendicular to the plane (i.e., to the long

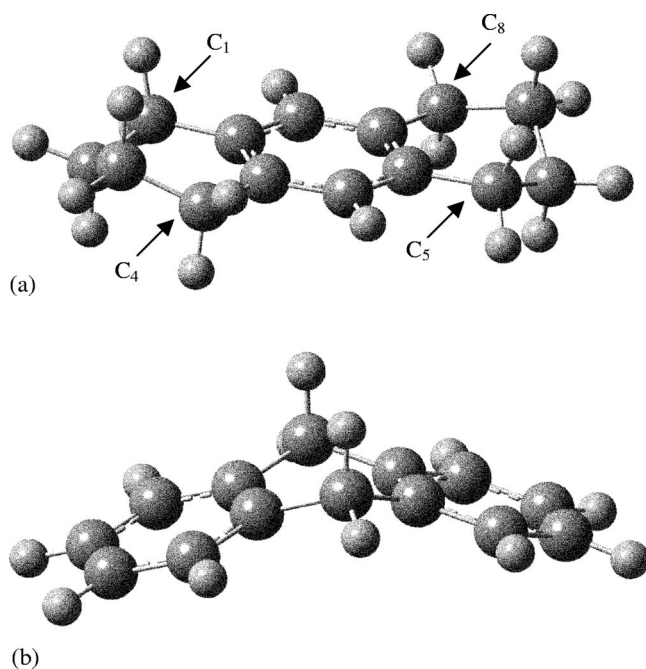


FIG. 7. Molecular structures of nonplanar molecules: (a) OHA and (b) DHA.

axis) of the molecule, whereas the $|g\rangle \rightarrow |CT\rangle$ transition dipole is directed along that long axis. Therefore, the electric field vector along this axis is most efficient in inducing the $|g\rangle \rightarrow |CT\rangle$ transition, not the $\pi \rightarrow \pi^*$ transition. By contrast, for a nonplanar molecule, there is no direction of the electric field that would selectively excite $|g\rangle \rightarrow |CT\rangle$ or $\pi \rightarrow \pi^*$ transitions.

With this in mind, we used in our study one nonplanar molecule, DHA, along with the other molecules, all of which are planar (OHA can be considered planar, in the sense of the current discussion). The DHA molecule has reduced symmetry, C_{2v} in comparison with the D_{2h} symmetry of anthracene, naphthalene, and tetracene. OHA has the carbon atoms 1, 4, 5, and 8 slightly twisted out of the aromatic plane, reducing the symmetry to D_2 ; see Fig. 7(a). However, the $|g\rangle \rightarrow |CT\rangle$ and $\pi \rightarrow \pi^*$ in this molecule are still orthogonal. In DHA, the two aromatic rings meet at the angle of $\sim 112^\circ$ due to sp^3 hybridized carbons 9 and 10, see Fig. 7(b). Due to this nonplanar structure, the CT transition should contain a significant contribution from the $\pi \rightarrow \pi^*$ transition. Indeed, our calculations show that for DHA the doorway transition dipole corresponds to a superposition of $|g\rangle \rightarrow |CT\rangle$ and $\pi \rightarrow \pi^*$ excitations.

The concept of $|DS\rangle$ state developed here will be of primary importance in calculating the fraction of dissociated ions as a function of laser intensity later in this paper. Good agreement of the results of these calculations with experimental data strongly supports the validity of the concept. This evidence is further corroborated by photoelectron spectra of polyatomic molecules [56], including some of the molecules used in this study. For example, in the ATI photoelectron spectra of benzene and naphthalene we observed two series of peaks separated by photon energy of the pulse (1.55

eV) that we attribute to π - π^* and CT excitations in these molecules (i.e., the states that are most strongly coupled to $|g\rangle$). Thus, the $|\text{DS}\rangle$ concept is a necessary element of a realistic model of nonadiabatic excitation of polyatomic molecules.

Once the $|\text{DS}\rangle$ state is identified, one can substitute the relevant values of μ and Δ in Eq. (3) to obtain the transition probabilities for comparison with the experimental data. However, as we see in the following subsection, Eq. (3) for $\Delta E_{|m\rangle,|n\rangle}(t)$ of the two-state model does not lead to satisfactory agreement with the experimental data.

B. Multistate model: Dynamic energy shift

To probe whether the two-state model is consistent with our fragmentation experiments, we calculated the half-laser-cycle probabilities for the $|g\rangle \rightarrow |\text{DS}\rangle$ transition at the laser intensities I_{fragm} , using Eq. (3). If the two-state model were adequate in describing these experiments, the results of these calculations would satisfy the following obvious criteria. First, to explain the onset of the extensive fragmentation at the laser intensity I_{fragm} , the calculated probabilities should be reasonably large. Second, the values of laser intensity corresponding to the same excitation probability should follow the order of relative stability of these molecules, as is the case with the experimental curves. Third, taking the measured intensity values corresponding to the same degree of fragmentation of different molecules and substituting them in the theoretical formulas for nonadiabatic excitation probability, one should obtain the same (within experimental uncertainty) probability values.

In drastic contrast to these expectations, the calculated probability values, listed in Table I, are very low, ranging from $\sim 3.8 \times 10^{-6}$ for OHA to $\sim 3.0 \times 10^{-2}$ for benzene. These values are too small to account even for the ionization of these molecules, let alone for the onset of extensive fragmentation. The probability values are not uniform—they vary by about four orders of magnitude. More importantly, the two-state calculation does not even reproduce the relative order of stability of these six molecules (i.e., for this set of molecules the two-state model does not work even qualitatively). For example, in the two-state model, OHA is predicted to be the most stable molecule, while the molecule that is the hardest to fragment in this experiment is benzene. Benzene, the most stable molecule, is predicted to have the highest probability of nonadiabatic excitation. Because these three criteria are not satisfied, we conclude that the two-state model does not adequately describe the coupling of $|g\rangle$ to the manifold of exciting states. Clearly, this model should be substantially revised to accommodate the complexity of real molecular structures.

One of the differences between a two-state and a multistate electronic system is that in the multistate system both $|g\rangle$ and $|\text{DS}\rangle$ states can couple not only to each other but also to many other states. Thus, the important fact neglected in the two-state model is that the shift of a given energy level in a low-frequency strong field is determined not only by the virtual transition to the most strongly coupled state, but also by polarization of the entire electronic system of the mol-

ecule. Indeed, the perturbative formula for the dynamic polarizability of $|g\rangle$ is

$$\alpha_g(\omega) = \sum_n \frac{(E_g - E_n) |\mu_{gn}|^2}{(E_g - E_n)^2 - \omega^2}, \quad (4)$$

where E_n is the energy of the n th state. Since in our case $\hbar\omega \ll \Delta_{|g\rangle \rightarrow |\text{DS}\rangle}$, the contribution of the $|\text{DS}\rangle$ state to the total polarizability of $|g\rangle$ reduces to $\mu_{|g\rangle \rightarrow |\text{DS}\rangle}^2 / \Delta_{|g\rangle \rightarrow |\text{DS}\rangle}$. The values of this contribution are compared with the values of total polarizability in Table I; they range from 74% for benzene to 4% for OHA. Since it is ultimately the total polarization of the electronic system that enables the $|g\rangle \rightarrow |\text{DS}\rangle$ transition, we must include this collective multielectron effect to describe the nonadiabatic excitation correctly.

When the Stark shift of the energy levels taken into account, the basic interlevel energy distance in Eq. (2) becomes electric-field-dependent, $\Delta_{mn} = \Delta_{mn}(\varepsilon(t))$. The specific form of this dependence at finite values of the oscillating electric field is determined by the mechanisms of the time-dependent energy change of the electronic states $|n\rangle$ and $|m\rangle$ (in our case, the $|g\rangle$ and the $|\text{DS}\rangle$ state). Since $|g\rangle$ is separated from the manifold of the excited states by the considerable energy gap $\Delta \gg \hbar\omega$, we assume that its energy variation in the electric field due to interaction with all the excited states with the exception of the $|\text{DS}\rangle$ state is described by the quasistatic formula

$$E_g(t) = E_g^{(0)} - \frac{1}{2} \left(\alpha_g - \frac{\mu_{|g\rangle \rightarrow |\text{DS}\rangle}^2}{\Delta_{|g\rangle \rightarrow |\text{DS}\rangle}} \right) \varepsilon^2(t). \quad (5)$$

We calculated the dynamic polarizabilities α_g at the laser frequency for all the participating molecules using the GAUSSIAN G01 development version program [46]; the obtained values are listed in Table I. Since these dynamic polarizabilities are only slightly greater than the static ones (by 1–3%), the quasistatic approach is justified.

Unlike the ground state, which is separated from the nearest excited state by an energy gap $\Delta \gg \hbar\omega$, the doorway state is surrounded by a dense manifold of excited states. The quasistatic approach to polarizability calculation is no longer valid in this situation. Just the opposite, the doorway state is in the high-frequency regime, because the laser photon energy $\hbar\omega = 1.55$ eV is much larger than the typical energy separation between the excited states, which is of the order of 0.1 eV. In this case, no quantum chemistry software package based on an adiabatic basis set can succeed in dynamic polarization calculations. Qualitatively, however, one can expect the dynamic polarizability of the doorway state to be negligibly small compared to that of the ground state. Indeed, among all the excited states contributing to the $|\text{DS}\rangle$ polarizability via virtual dipole transitions in Eq. (4), the major contribution comes from the energy region $E_n - E_{\text{DS}} \sim \hbar\omega$. In the dense manifold of the excited states, the transition dipole is a smooth function of n . Thus, the contributions of the states with $E_n - E_{\text{DS}} > \hbar\omega$ and the states with $E_n - E_{\text{DS}} < \hbar\omega$ almost cancel each other [57]. Following these arguments, we conclude that

$$\Delta(t) = E_{\text{DS}}(t) - E_g(t) = E_{\text{DS}}^{(0)} - E_g^{(0)} + \frac{1}{2} \left(\alpha_g - \frac{\mu_{|g\rangle \rightarrow |\text{DS}\rangle}^2}{\Delta_{|g\rangle \rightarrow |\text{DS}\rangle}} \right) \varepsilon^2(t). \quad (6)$$

Then, the equation for the time-dependent transition energy from $|g\rangle$ to $|\text{DS}\rangle$, incorporating the effect of all electrons on the Stark shift of these states, expressed through the polarizability, is

$$\Delta E_{|g\rangle, |\text{DS}\rangle}(t) = \sqrt{\left(\Delta_0 + \frac{\alpha_g^*}{2} \varepsilon^2(t) \right)^2 + 4\mu^2 \varepsilon^2(t)}. \quad (7)$$

Here, the effective dynamic polarization of $|g\rangle$, α_g^* , excludes the contribution from the $|\text{DS}\rangle$ state,

$$\alpha_g^* = \alpha_g - \frac{\mu_{|g\rangle \rightarrow |\text{DS}\rangle}^2}{\Delta_{|g\rangle \rightarrow |\text{DS}\rangle}}. \quad (8)$$

This leads to the formula for the probability of the nonadiabatic transition per half-laser cycle in a multistate electronic system,

$$P_{|g\rangle \rightarrow |\text{CT}\rangle} = \exp \left[- \frac{\pi \Delta_0^2}{4\hbar \omega \varepsilon_0 \sqrt{\mu^2 + \frac{\alpha_g^* \Delta_0}{4}}} \right]. \quad (9)$$

C. Sequential excitation in molecular ions

The nonadiabatic excitation of neutral molecules is not sufficient to account for the laser intensity dependence of dissociative ionization. Indeed, the onset and even saturation of nonadiabatic excitation of a neutral molecule does not immediately and automatically result in the formation of ionized fragments. For the short pulses used here, ionization of the original molecule must occur during the laser pulse, i.e., prior to its fragmentation. In our experiments, we observe that within some range of the laser intensities (specific for a given molecule), the laser pulses produce predominantly parent molecular ions. Whether and how the fragmentation will proceed must depend on the extent of nonadiabatic excitation of the molecular ion.

To understand and quantitatively describe the relation of the excitation process and the fragmentation outcome, we propose the following two-stage scenario. At the first stage, the $|g\rangle \rightarrow \text{QC}$ nonadiabatic transition in a neutral molecule is followed by fast energy absorption within the QC resulting in ionization (energy deposition within the QC is much more probable than promotion of another electron to the QC through the $|\text{DS}\rangle$). Thus, the $|g\rangle \rightarrow |\text{DS}\rangle$ population transfer described in the previous section is the bottleneck step in the energy deposition in neutral molecules resulting in single ionization. Because the ionized electron takes away most of the energy gained by the molecule prior to ionization, the molecular ion is formed in a relatively cold state. (Here, we exclude the exotic scenario of ionization through highly excited autoionized states.) To access the repulsive states in the ionic quasicontinuum, QC_i , the bottleneck for the transition

from the ionic ground state, $|g_i\rangle$, to QC_i must be overcome. Then, the observed fragmentation requires additional excitation of these ions in the QC_i .

At the second stage, nonadiabatic $|g_i\rangle \rightarrow \text{QC}_i$ transition in the molecular ion provides access to the repulsive electronic states, resulting in the formation of the detected ionic fragments. The $|g_i\rangle \rightarrow \text{QC}_i$ transition in molecular ions is conceptually the same as that in neutral molecules: the ionic $|g_i\rangle$ state is most strongly coupled to the doorway state in the ionic excited-state manifold, $|\text{DS}_i\rangle$ (in the case of these molecules, the lowest charge-resonance state of the ion); the probability of the $|g_i\rangle \rightarrow |\text{DS}_i\rangle$ transition is significantly increased by the dynamic polarizability of the ion.

However, the dynamic polarizability of large molecular ions is qualitatively different from that of neutral molecules because in an ion there is a number of low-energy electronic transitions, corresponding to an electron hole migrating through the orbitals below the highest occupied molecular orbital (HOMO). Such nominally $\pi \rightarrow \pi$, $\sigma \rightarrow \pi$, and $\sigma \rightarrow \sigma$ transitions typically belong to the visible or near-infrared range of the spectrum. These transitions have no analog in neutral molecules (they are forbidden in closed-shell systems by the Pauli exclusion principle). The effect of these sub-HOMO transitions is that in Eq. (9) the energy gap Δ_0 becomes smaller while the polarizability α^* becomes larger, compared to the values for the neutral molecule. Both factors lead to an exponential enhancement of the nonadiabatic transition probability.

To substantiate this qualitative difference in polarizabilities of molecules and molecular ions, we have calculated a considerable number (20–50) of energy levels (up from the ground state) of a neutral molecule and a corresponding molecular ion for all of the participating molecules. The results are presented in Fig. 8; they clearly indicate the drastic difference in the structure of low-lying levels of the molecules and the ions. An excited state, $|g_i\rangle$, is accompanied by a number of nearby states, in contrast to the solitude of the $|g\rangle$ state of a neutral molecule. Thus, a number of low-energy transitions between these states is readily available to increase the ionic polarizability. This can be seen in the $|g_i\rangle$ polarizabilities listed in Table I. With the exception of benzene (the smallest molecule) and DHA (the only nonplanar molecule in this series), the polarizabilities of the molecular ions are greater (for tetracene significantly greater) than those of the corresponding neutral molecules.

We note in passing that the increase of the polarizability as a result of ionization that we observe for the larger molecules, compared to the opposite effect for benzene, signifies a general trend relevant to all large molecules. Qualitatively, two competing factors contribute predominantly to the change of polarizability following ionization: (a) opening of the previously mentioned electron-hole dynamics, and (b) reduction of the number of electrons available for polarization. Since the first factor is definitely more pronounced in large molecules and the second in small molecules, large molecular ions will usually have polarizability greater than the corresponding neutral molecule, with the opposite result in the case of small ions [55].

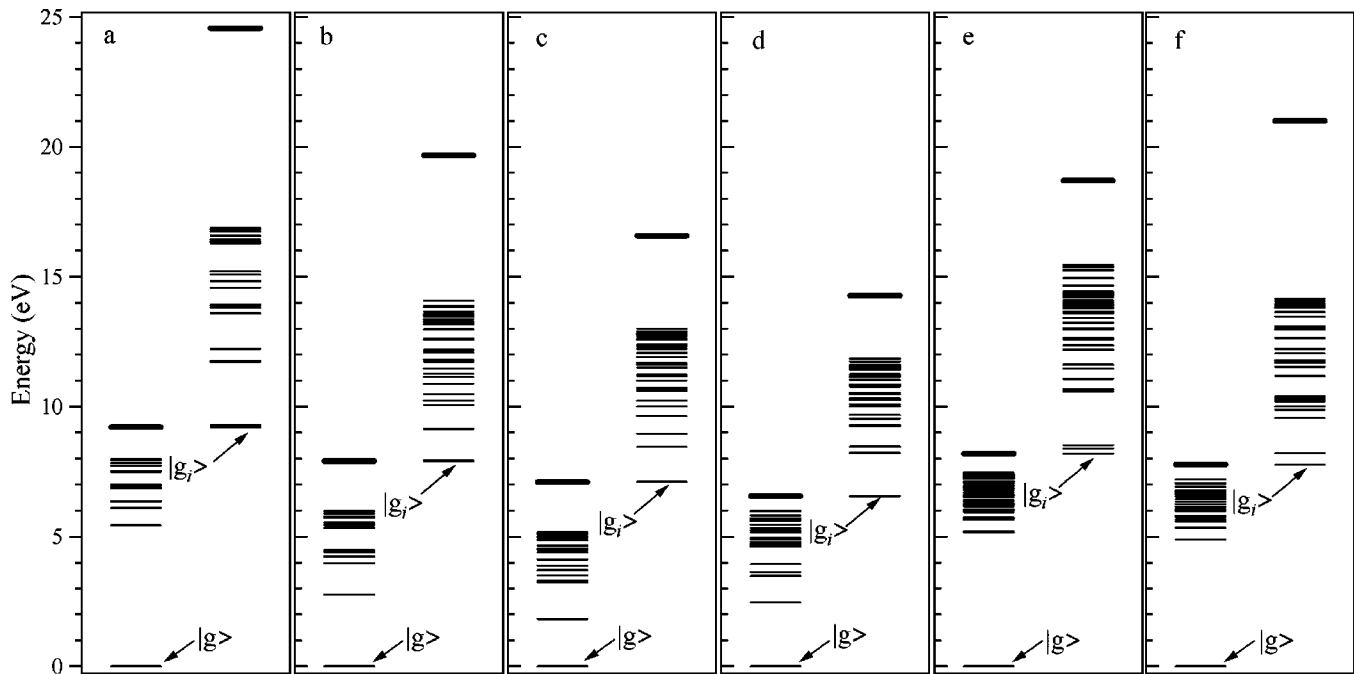


FIG. 8. Low-lying electronic states of benzene, naphthalene, anthracene, tetracene, DHA, and OHA calculated for both neutral molecules and molecular ions using the GAUSSIAN 01 (development version) computer program using the B3LYP density-functional method with 6-31+G(d) basis set.

The additional electronic transitions contribute substantially to the dynamic polarization of large polyatomic ions and significantly affect energy deposition. Using the electronic properties of the ions listed in Table I, we can calculate the probability of the $|g_i\rangle \rightarrow \text{QC}_i$ excitation for each ion. Finally, we combine the three essential elements of our model: (i) the doorway transition to QC through a $|\text{CT}\rangle$ state, (ii) the multielectron polarization, and (iii) the ion excitation, into a two-stage nonadiabatic excitation calculation that can be compared with the measured fraction of the dissociated ions shown in Figs. 4(a) and 4(b).

As in the case of transition to a true continuum [43], the total excitation probability is obtained by summation of the conditional probabilities over half-cycles of the laser pulse. By the m th half-cycle of the pulse, the total excitation probability for a neutral molecule is

$$P_{\text{total}}^{\text{neut}}(m) = 1 - \prod_{n=1}^m [1 - P_{|g\rangle \rightarrow |\text{CT}\rangle}(n)], \quad (10)$$

where the dependence $P_{|g\rangle \rightarrow |\text{CT}\rangle}(n)$ on the cycle number, n , is determined by the envelope $\varepsilon_0^2(n)$. In the two-stage calculation, the nonadiabatic excitation in neutral molecules produces ionization. Then, the fraction of dissociated ions is computed as the sum of conditional probabilities of the parent ion excitation $P_{|g_i\rangle \rightarrow \text{QC}_i}$ over the rest of the laser pulse [similar to Eq. (10)], normalized by the ionization probability. Thus, for a pulse containing N half-cycles, the fraction of dissociated ions is

$$P_{\text{total}} = \sum_{m=1}^N P_{\text{total}}^{\text{ion}}(N-m) P_{\text{total}}^{\text{neut}}(m). \quad (11)$$

The calculation of the fractions of ions fragmented as a function of laser intensity, shown in Figs. 4(a) and 4(b) by the solid curves, agrees well with the experimental data on the fragmented ion fractions. The calculated curves reproduce the order of relative stability of these molecules against fragmentation. The curves reproduce the increase in the slope with increasing size of a molecule (or increasing extent of π -electron delocalization for molecules of similar size). The curves predict quantitatively the range of laser intensities where each molecule is expected to undergo extensive fragmentation. This agreement, achieved with no fitting parameters in the theory, strongly suggests that the three elements of our model of nonadiabatic excitation of polyatomic molecules capture the most important features of nonresonant laser/molecule coupling leading to dissociative ionization. The remaining discrepancy at high laser intensities (near the saturation limit) is most likely caused by multiple ionization. (If at high laser intensities the sequential excitation includes more than two stages, the amount of detected ionic fragments will be greater than predicted by the two-stage model.)

V. CONCLUSIONS

Before summarizing our findings, we note that the model of dissociative ionization by sequential nonadiabatic excitation developed here is directly relevant to many other phenomena in the field of laser-induced transformations of polyatomic molecules. The model can address the interplay of neutral fragmentation channels [3] (the channels dark to ion detection), intact ionization, and ionized fragmentation channels. In particular, the electronic absorption by polyatomic ions at the fundamental laser wavelength (800 nm) is re-

ported to significantly enhance the ion fragmentation [58]. These IR electronic transitions, related to the above-mentioned electron-hole dynamics, do not involve the high-energy repulsive states and thus cannot by themselves induce the ion dissociation. However, the increase in the ion polarizability due to the existence of these transitions will boost the $|g_i\rangle \rightarrow \text{QC}_i$ transition probability [see Eq. (7)], enhancing the ion fragmentation.

Of course, to be capable of quantitative predictions in more complex cases, this theory requires further development. Currently, the model addresses the processes of nonadiabatic excitation; redistribution of the deposited energy over the molecular degrees of freedom is beyond the scope. To be helpful in cases of multiple possible outcomes, the model needs to address the complex coupling of electronic states within the QC and to incorporate the interaction between the electron excitation and the nuclear motion. With this, the essential effects of the laser pulse duration can be addressed, such as ladder climbing versus ladder switching modes of excitation [59]. The model can also address the differences between cyclic and aliphatic molecules with regard to neutral fragmentation versus dissociative ionization outcomes. The nonadiabatic charge-transfer transitions enhanced by multielectron polarization are undoubtedly important for understanding of the processes of high harmonic generation [60,61] in large molecules.

A further improvement of this model would more accurately account for the $|\text{CT}\rangle$ state polarization dynamics. When the density of states surrounding the excited $|\text{CT}\rangle$ state is not large enough (or the field frequency is not high enough), the dynamic polarizability of this state may become non-negligible. In this situation, the time-dependent energy of the $|\text{CT}\rangle$ state will be determined by a complex interplay of its own built-in dipole and the details of coupling to the nearby states. This may affect the estimates of the nonadiabatic transition probability. Thus, an appropriate analytical model and concurrent numerical approach to the strong-field dynamic Stark effect in polyatomic molecules is the natural next step in the development of this theory.

In summary, by measuring the laser intensity thresholds for fragmentation as a function of molecular size, symmetry, and electronic structure, we have identified the physical mechanism of energy deposition leading to dissociative ionization in a number of polyatomic molecules. We have developed a general theory for dissociative ionization of polyatomic molecules in strong nonresonant fields that is based on sequential nonadiabatic excitation of a molecule and the resulting molecular ions. The three key elements of the model are (i) nonadiabatic population transfer from $|g\rangle$ to the excited-state manifold via a doorway charge-transfer (CT) transition; (ii) exponential enhancement of this transition by collective dynamic polarization of all electrons, and (iii) sequential energy deposition in the neutral molecules and corresponding molecular ions, resulting in the formation of ionized fragments. Based on this model, we calculated the fragmentation probabilities that agree quantitatively with the experimental data. We propose that this model represents a generic sequential excitation process, consisting (at the onset of extensive fragmentation) of two stages. At the first stage,

the nonadiabatic excitation of neutral molecules occurs and results in the formation of relatively cold molecular ions. At the second stage, the nonadiabatic excitation of the ions provides a sufficient amount of energy to break molecular bonds, resulting in eventual fragmentation. The latter outcome is determined by the details of the ionic energy-level structure. In this regard, nonadiabatic electron dynamics of large polyatomic molecules is drastically different from that of atoms and small molecules. Namely, the ionization of a small molecule typically decreases its polarizability and slows the rate of nonadiabatic excitation, whereas for a large molecule the opposite is true, leading to avalanche excitation, which correlates well with experimental observations. Further development of this theory is expected to provide a basis for strong-field control of ionization, fragmentation, and chemical reactions of polyatomic molecules in gas and liquid phase.

ACKNOWLEDGMENTS

The authors would like to gratefully acknowledge the financial support of NSF, ONR, and the DOD MURI program as administered by the Army Research Office.

APPENDIX: NONADIABATIC ELECTRONIC TRANSITIONS ASSISTED BY STARK SHIFT

According to the Dykhne approximation [43], the transition amplitude A_{mn} between the eigenstates $|n\rangle$ and $|m\rangle$ of a two-level system is

$$A_{mn} = i \exp \left[\frac{i}{\hbar} \left\{ \int_{t_1}^{\tau} \Delta E_{mn}(t) dt \right\} \right], \quad (\text{A1})$$

where t_1 is a point on the real time axis and τ is a point in the upper half-plane of the complex variable t such that $E_n(\tau) = E_m(\tau)$. The $\Delta E_{mn}(t)$ here is the time-dependent energy separation of the eigenstates. In a monochromatic electric field $\varepsilon(t) = \varepsilon_0 \sin(\omega t)$, the dependence $\Delta E_{mn}(t)$ on t is caused by (i) the dipole coupling of the states $|n\rangle$ and $|m\rangle$, $\mu \varepsilon(t)$, and (ii) the regular Stark shift induced by all the other states of the multistate system,

$$E_n^{\text{field}} = E_n^0 - \frac{\alpha_n(\omega)}{2} \varepsilon^2(t),$$

$$E_m^{\text{field}} = E_m^0 - \frac{\alpha_m(\omega)}{2} \varepsilon^2(t), \quad (\text{A2})$$

where $\alpha_n(\omega)$ and $\alpha_m(\omega)$ are the dynamic polarizabilities of the $|n\rangle$ and $|m\rangle$ states. Therefore, the energy spacing between these states becomes

$$\Delta E_{mn}(t) = E_m(t) - E_n(t)$$

$$= \sqrt{\left(\Delta_0 + \frac{\delta\alpha(\omega)}{2} \varepsilon^2(t) \right)^2 + 4\mu^2 \varepsilon^2(t)}, \quad (\text{A3})$$

where $\delta\alpha(\omega)$ is the difference of the dynamic polarizabilities. The term $1/4\delta\alpha^2(\omega)\varepsilon^4(t)$ being small comparing to others, the $\Delta E_{mn}(t)$ becomes

$$\Delta E_{mn}(t) = \sqrt{\Delta_0^2 + [4\mu^2 + \delta\alpha(\omega)\Delta_0]\varepsilon^2(t)} \quad (\text{A4})$$

resulting in

$$A_{mn} = \exp\left[\frac{i}{\hbar} \int_0^{\tau_0} \sqrt{\Delta_0^2 + [4\mu^2 + \delta\alpha(\omega)\Delta_0]\varepsilon^2(t)} dt\right]. \quad (\text{A5})$$

Changing the dummy variable, $u = -i\omega t$, we obtain

$$A_{mn} = \exp\left[-\frac{1}{\hbar\omega} \int_0^{u_0} \sqrt{p - q \sinh^2(u)} du\right], \quad (\text{A6})$$

where

$$p = \Delta_0^2; \quad q = [4\mu^2 + \delta\alpha(\omega)\Delta_0]\varepsilon_0^2. \quad (\text{A7})$$

For strong laser fields, the transition occurs when $4\mu^2\varepsilon_0^2 \gg \Delta_0^2$ ($q \gg p$), i.e., for small values of u , where

$$\sinh^2(u) \approx u^2. \quad (\text{A8})$$

This approximation leads to

$$\begin{aligned} A_{mn} &= \exp\left[-\frac{\sqrt{p}}{\hbar\omega} \int_0^{u_0} \sqrt{1 - \frac{q}{p}u^2} du\right] \\ &= \exp\left[-\frac{p}{\hbar\omega\sqrt{q}} \left(\frac{z}{2} \sqrt{1-z^2} + \sin^{-1}(z)\right)\right]_{z=0}^{z=1} \\ &= \exp\left[-\frac{\pi p}{4\hbar\omega\sqrt{q}}\right]. \end{aligned} \quad (\text{A9})$$

Finally, the probability of a nonadiabatic transition in strong field during a half-laser cycle is obtained as

$$P_{mn} = |A_{mn}|^2 = \exp\left[-\frac{\pi\Delta_0^2}{4\hbar\omega\varepsilon_0 \sqrt{\mu^2 + \frac{\delta\alpha(\omega)\Delta_0}{4}}}\right]. \quad (\text{A10})$$

Note that the assumption of small u [Eq. (8)] is satisfied much better after the introduction of the differential Stark shifting of the energy levels in a multistate system.

-
- [1] M. J. DeWitt and R. J. Levis, *Phys. Rev. Lett.* **81**, 5101 (1998).
 [2] M. J. DeWitt and R. J. Levis, *J. Chem. Phys.* **102**, 8670 (1995).
 [3] M. J. DeWitt, D. W. Peters, and R. J. Levis, *Chem. Phys.* **218**, 211 (1997).
 [4] C. Kosmidis *et al.*, *J. Phys. Chem. A* **103**, 6950 (1999).
 [5] E. E. B. Campbell *et al.*, *J. Chem. Phys.* **114**, 1716 (2001).
 [6] A. Talebpour, S. Larochele, and S. L. Chin, *J. Phys. B* **31**, 2769 (1998).
 [7] L. J. Frasinski, K. Codling, and P. A. Hatherly, *Science* **246**, 1029 (1989).
 [8] L. J. Frasinski *et al.*, *Phys. Rev. Lett.* **58**, 2424 (1987).
 [9] M. Boyle *et al.*, *Phys. Rev. Lett.* **87**, 273401 (2001).
 [10] N. A. Anderson, J. J. Shiang, and R. J. Senson, *J. Phys. Chem. A* **103**, 10730 (1999).
 [11] N. A. Anderson *et al.*, *Chem. Phys. Lett.* **323**, 365 (2000).
 [12] M. J. DeWitt and R. J. Levis, *J. Chem. Phys.* **108**, 7739 (1998).
 [13] A. N. Markevitch, N. P. Moore, and R. J. Levis, *Chem. Phys.* **267**, 131 (2001).
 [14] R. J. Levis, G. M. Menkir, and H. Rabitz, *Science* **292**, 709 (2001).
 [15] A. Assion *et al.*, *Science* **282**, 919 (1998).
 [16] R. J. Levis and H. A. Rabitz, *J. Phys. Chem.* **106**, 6427 (2002).
 [17] L. V. Keldysh, *Sov. Phys. JETP* **20**, 1307 (1965).
 [18] A. M. Perelomov, V. S. Popov, and M. V. Terent'ev, *Sov. Phys. JETP* **23**, 924 (1966).
 [19] M. V. Ammosov, N. B. Delone, and V. P. Krainov, *Sov. Phys. JETP* **64**, 1191 (1986).
 [20] W. C. Liu *et al.*, *Phys. Rev. Lett.* **83**, 520 (1999).
 [21] P. F. Agostini, F. Fabre, G. Mainfray, G. Petite, and N. K. Rahman, *Phys. Rev. Lett.* **42**, 1127 (1979).
 [22] M. P. Deboer and H. G. Muller, *Phys. Rev. Lett.* **68**, 2747 (1992).
 [23] R. R. Freeman *et al.*, *Phys. Rev. Lett.* **59**, 1092 (1987).
 [24] G. N. Gibson, R. R. Freeman, and T. J. McIlrath, *Phys. Rev. Lett.* **69**, 1904 (1992).
 [25] G. N. Gibson *et al.*, *Phys. Rev. A* **49**, 3870 (1994).
 [26] R. S. Mulliken, *J. Chem. Phys.* **7**, 20 (1939).
 [27] P. Dietrich and P. B. Corkum, *J. Chem. Phys.* **97**, 3187 (1992).
 [28] T. Seideman, M. Y. Ivanov, and P. B. Corkum, *Phys. Rev. Lett.* **75**, 2819 (1995).
 [29] D. M. Villeneuve, M. Y. Ivanov, and P. B. Corkum, *Phys. Rev. A* **54**, 736 (1996).
 [30] T. Zuo and A. D. Bandrauk, *Phys. Rev. A* **52**, R2511 (1995).
 [31] T. Zuo and A. D. Bandrauk, *Phys. Rev. A* **48**, 3837 (1993).
 [32] G. N. Gibson *et al.*, *Phys. Rev. A* **58**, 4723 (1998).
 [33] C. L. Guo, M. Li, and G. N. Gibson, *Phys. Rev. Lett.* **82**, 2492 (1999).
 [34] C. Ellert and P. B. Corkum, *Phys. Rev. A* **59**, R3170 (1999).
 [35] M. Lezius *et al.*, *Phys. Rev. Lett.* **86**, 51 (2001).
 [36] A. N. Markevitch *et al.*, *Phys. Rev. A* **68**, 011402 (2003).
 [37] M. J. DeWitt and R. J. Levis, *J. Chem. Phys.* **110**, 11368 (1999).
 [38] R. J. Levis and M. J. DeWitt, *J. Phys. Chem. A* **103**, 6493 (1999).
 [39] M. A. Walker, P. Hansch, and L. D. Van Woerkom, *Phys. Rev. A* **57**, R701 (1998).
 [40] T. D. G. Walsh *et al.*, *J. Phys. B* **27**, 3767 (1994).
 [41] M. J. DeWitt and R. J. Levis, *J. Chem. Phys.* **108**, 7045 (1998).
 [42] M. M. Murnane *et al.*, *Science* **251**, 531 (1991).
 [43] N. B. Delone and V. P. Krainov, *Atoms in Strong Laser Fields* (Springer-Verlag, Berlin, 1985), Chap. 4.
 [44] L. Allen and J. H. Eberly, *Optical Resonance and Two-level Atom* (Wiley, New York, 1975), Chap. 3.

- [45] N. B. Delone and V. P. Krainov, *Atoms in Strong Laser Fields* (Springer-Verlag, Berlin, 1985).
- [46] M. J. Frisch *et al.*, GAUSSIAN 01 (Gaussian, Inc., Pittsburgh, PA, 2000).
- [47] A. D. Becke, Phys. Rev. A **38**, 3098 (1988).
- [48] A. D. Becke, J. Chem. Phys. **98**, 5648 (1993).
- [49] C. T. Lee, W. T. Yang, and R. G. Parr, Phys. Rev. B **37**, 785 (1988).
- [50] A. J. H. Wachters, J. Chem. Phys. **52**, 1033 (1970).
- [51] J. P. Hay, J. Chem. Phys. **66**, 4377 (1977).
- [52] R. Krishnan *et al.*, J. Chem. Phys. **72**, 650 (1980).
- [53] A. D. McLean and G. S. Chandler, J. Chem. Phys. **72**, 5639 (1980).
- [54] K. Raghavachari and G. W. Trucks, J. Chem. Phys. **91**, 1062 (1989).
- [55] S. M. Smith *et al.*, (unpublished).
- [56] A. N. Markevitch, A. D. Romanov, and R. J. Levis (unpublished).
- [57] V. M. Akulin and N. V. Karlov, *Intense Resonant Interactions in Quantum Electronics* (Springer-Verlag, Berlin, 1992).
- [58] H. Harada *et al.*, Chem. Phys. Lett. **342**, 563 (2001).
- [59] R. Weinkauf *et al.*, J. Phys. Chem. **98**, 8381 (1994).
- [60] M. Lein *et al.*, Phys. Rev. Lett. **88**, 183903 (2002).
- [61] R. Velotta *et al.*, Phys. Rev. Lett. **87**, 183901 (2001).